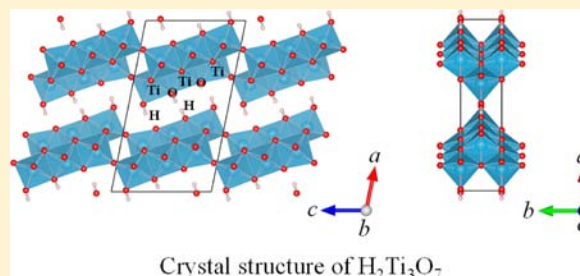


Ion-Exchange Synthesis, Crystal Structure, and Physical Properties of Hydrogen Titanium Oxide $\text{H}_2\text{Ti}_3\text{O}_7$ Kunimitsu Kataoka,^{*,†} Norihito Kijima,[†] and Junji Akimoto^{*,†}[†]National Institute of Advanced Industrial Science and Technology (AIST), 1-1-1 Higashi, Tsukuba, Ibaraki 305-8565, Japan

Supporting Information

ABSTRACT: Hydrogen titanium oxide $\text{H}_2\text{Ti}_3\text{O}_7$ was prepared from $\text{Na}_2\text{Ti}_3\text{O}_7$ as a parent compound via Na^+/H^+ ion exchange in acidic solution at 333 K. It crystallizes in the monoclinic system, space group $C2/m$, and the lattice parameters of $a = 16.0380(8)$ Å, $b = 3.7533(1)$ Å, $c = 9.1982(3)$ Å, and $\beta = 101.414(3)^\circ$. The crystal structure of $\text{H}_2\text{Ti}_3\text{O}_7$ was refined to the conventional values of $R_{\text{wp}} = 2.60\%$ and $R_p = 1.97\%$ with a fit indicator of $\text{GOF} = R_{\text{wp}}/R_e = 1.90$ by Rietveld analysis using powder neutron diffraction data. The basic $(\text{Ti}_3\text{O}_7)^{2-}$ framework in $\text{H}_2\text{Ti}_3\text{O}_7$ was changed from that in the parent $\text{Na}_2\text{Ti}_3\text{O}_7$. The atomic coordinate of hydrogen atoms were determined by this study for the first time. The hydrogen site in the layer space was refined with a strict H1–O3 distance of $0.80(2)$ Å and H2–O4 distance of $0.86(2)$ Å in $\text{H}_2\text{Ti}_3\text{O}_7$, respectively. The structural stability of $\text{H}_2\text{Ti}_3\text{O}_7$ was confirmed by bond valence sums. From these results, protons were suggested as the ordered occupation in the crystal structure.

Crystal structure of $\text{H}_2\text{Ti}_3\text{O}_7$

INTRODUCTION

Hydrogen titanium oxides display a wide range of interesting chemical and electrochemical properties. Two kinds of structure types are well-known in the $\text{H}_2\text{Ti}_3\text{O}_7$ composition; one is the ramsdellite-type, which is very attractive as a suitable electrolyte for low-temperature fuel cells for energy production,^{1–3} and the other has the layered $\text{Na}_2\text{Ti}_3\text{O}_7$ related-type crystal structure.^{4–6} These compounds can be prepared by soft-chemical synthetic route using alkali titanates of $\text{Li}_2\text{Ti}_3\text{O}_7$ and $\text{Na}_2\text{Ti}_3\text{O}_7$ as parent compounds.

Izawa, Kikkawa and Koizumi first reported hydrogen titanium oxide, $\text{H}_2\text{Ti}_3\text{O}_7$; this compound was prepared from $\text{Na}_2\text{Ti}_3\text{O}_7$ at 333 K for 3 days by the Na^+/H^+ ion-exchange.⁴ Faist and Davis reported reinvestigation of the synthetic condition and refinement of crystal structure by neutron diffraction.⁶ The basic $(\text{Ti}_3\text{O}_7)^{2-}$ framework in $\text{H}_2\text{Ti}_3\text{O}_7$ was maintained nearly unchanged from that in parent $\text{Na}_2\text{Ti}_3\text{O}_7$. However hydrogen positions were not determined. Recently, the thermoanalysis, the electrochemical property and hydrogen information by spectroscopy of $\text{H}_2\text{Ti}_3\text{O}_7$ was reported by Akimoto et al.⁷ They suggested two types of hydrogen sites in structure by ^1H MAS NMR, however, detailed sites could not determine. The structural details of $\text{H}_2\text{Ti}_3\text{O}_7$, especially the H atomic positions, have not been revealed yet, to the best of our knowledge, in spite of interests in the one-dimensional proton conduction property, as in the case of the ramsdellite-type $\text{H}_2\text{Ti}_3\text{O}_7$.³

The present study has three main objectives. First, we determined the precise crystal structure of $\text{H}_2\text{Ti}_3\text{O}_7$ by powder neutron diffraction technique. Second, we clarified preliminary physical properties of $\text{H}_2\text{Ti}_3\text{O}_7$, in comparison with those of the related titanate compounds.

EXPERIMENTAL SECTION

Sample Preparation. In the present study, the sample preparation was performed by three synthetic steps. First, the precursor $\text{Na}_2\text{Ti}_3\text{O}_7$ was prepared by a conventional solid state reaction, as previously reported.^{4–8} A mixture of Na_2CO_3 (99.9% pure) and TiO_2 (99.99% pure) in a molar ratio of 1:3 was heated at 1073 K for 20 h in air. The resultant specimens were reground, and the same temperature program sequence was repeated once again. Then, the layered $\text{H}_2\text{Ti}_3\text{O}_7$ sample was prepared from $\text{Na}_2\text{Ti}_3\text{O}_7$ via Na^+/H^+ ion exchange reaction using a 0.5 M HCl solution for 5 days at 333 K, as previously reported.^{4–7} After the acidic treatment, the produced $\text{H}_2\text{Ti}_3\text{O}_7$ samples was washed with water and ethanol, and then dried at 333 K for 1 day in air.

Chemical Characterization. The phase purity and crystal structure of the obtained sample was characterized by powder X-ray diffraction (XRD) using a Rigaku RINT2550 V diffractometer (Cu $K\alpha$ radiation, operating conditions: 40 kV, 200 mA) equipped with a curved graphite monochromator. The XRD intensity data for the Rietveld analysis were collected for 1 s at each 0.03° step over a 2θ range from 5 to 140° .

The chemical analysis of Na and Ti contents was performed by inductive coupled plasma (ICP) spectroscopy (Varian 730-ES).

Crystal Structure Determination. The Rietveld refinement of $\text{H}_2\text{Ti}_3\text{O}_7$ was performed by Jana2006⁹ using powder neutron diffraction (ND) data measured at room temperature with wavelength $\lambda = 1.8024$ Å using a HERMES diffractometer (JAEA, JRR3M beamline T1–3).¹⁰ The ND intensity data collected for 0.05° step over a 2θ range from 7 to 157° .

The nuclear scattering length density distribution (NSLDD) analysis was performed by the maximum entropy method (MEM) based on the Rietveld analysis using the powder ND data. The MEM calculation was carried out with the unit cell divided into $128 \times 128 \times$

Received: May 10, 2013

Published: November 21, 2013

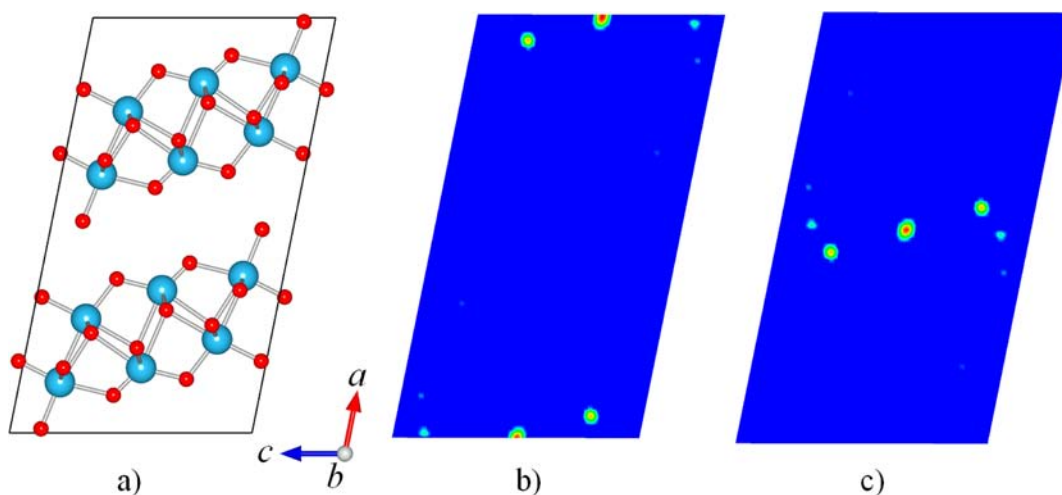


Figure 1. (a) The $(\text{Ti}_3\text{O}_7)^{2-}$ framework in the $\text{H}_2\text{Ti}_3\text{O}_7$ structure. The solid box indicates the unit cell. (b, c) Two-dimensional difference Fourier synthesis maps of $\text{H}_2\text{Ti}_3\text{O}_7$ using the powder ND data of the $y = 0$ and $y = 0.5$ sections, respectively. The negative residual nuclear scattering length density distributions for the H atoms are clearly observed in these maps.

128 pixels using a MEM analysis program PRIMA.¹¹ The crystal structure and MEM images were drawn using a computer program VESTA.¹²

Physical Property Measurements. AC impedance measurement for $\text{H}_2\text{Ti}_3\text{O}_7$ was conducted using a Solartron 1260 impedance analyzer operating at 10 mV applied ac amplitude at 13 MHz to 10 Hz frequencies at room temperature in air. In the present study, the measurements were performed using the powder sample of 89.90 mg under the pressure of 1.5 MPa with the relative density of about 70%. The size of the measurement holder was 10 mm in diameter and 0.5 mm thickness.

Optical absorption (UV–vis) spectrum was measured using a Jasco V-550 spectrometer over the range 300–600 nm at room temperature by diffuse reflection method. From the intersection values of the baseline and absorption band edge in the obtained spectra, we estimated the band gap energy of $\text{H}_2\text{Ti}_3\text{O}_7$.

RESULTS AND DISCUSSION

Ion-Exchange Synthesis of $\text{H}_2\text{Ti}_3\text{O}_7$. The obtained precursor sample was identified to be a single phase of $\text{Na}_2\text{Ti}_3\text{O}_7$, monoclinic crystal system, and the space group $P2_1/m$. No impurity phases were observed in the XRD patterns. The

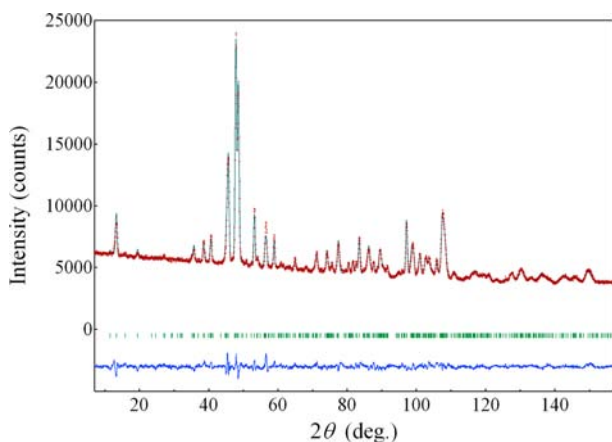


Figure 2. Observed, calculated, and difference patterns for the Rietveld refinement using the powder neutron diffraction data of $\text{H}_2\text{Ti}_3\text{O}_7$. The short vertical lines below the profiles mark positions of all position Bragg reflections of $\text{H}_2\text{Ti}_3\text{O}_7$.

Table 1. Atomic Coordinates and Isotropic Atomic Displacement Parameters (\AA^2) for $\text{H}_2\text{Ti}_3\text{O}_7$ Determined using the Powder ND Data

atom	site	occ.	<i>x</i>	<i>y</i>	<i>z</i>	U_{iso} (\AA^2)
H1	4i	1	0.4720(12)	0.5	0.4578(23)	0.059(4)
H2	4i	1	0.5439(13)	0.5	0.1850(21)	0.059(4)
Ti1	4i	1	0.2333(8)	0	0.2236(14)	0.0023(14)
Ti2	4i	1	0.1643(9)	0	0.4992(14)	0.0023(14)
Ti3	4i	1	0.1259(8)	0	0.8291(11)	0.0023(14)
O1	4i	1	0.1694(5)	0	0.0316(10)	0.0048(4)
O2	4i	1	0.1345(5)	0	0.3205(10)	0.0048(4)
O3	4i	1	0.0740(7)	0	0.5943(11)	0.0048(4)
O4	4i	1	0.0091(5)	0	0.8553(9)	0.0048(4)
O5	4i	1	0.3512(5)	0	0.1746(8)	0.0048(4)
O6	4i	1	0.2964(5)	0	0.4616(10)	0.0048(4)
O7	4i	1	0.2394(5)	0	0.7513(9)	0.0048(4)

Table 2. Selected Bond Distances (\AA) for $\text{H}_2\text{Ti}_3\text{O}_7$

H1–O3	0.80(2)		
H2–O4	0.86(2)		
Ti1–O1	1.85(2)	Ti1–O2	1.97(2)
Ti1–O5	2.03(2)	Ti1–O6	2.22(1)
Ti1–O7 × 2	1.931(3)		
Ti2–O2	1.62(1)	Ti2–O3	1.83(1)
Ti2–O6 × 2	1.990(4)	Ti2–O6	2.21(2)
Ti2–O7	2.39(2)		
Ti3–O1	1.86(1)	Ti3–O3	2.16(1)
Ti3–O4	1.93(2)	Ti3–O5 × 2	1.914(3)
Ti3–O7	2.08(1)		

lattice parameters for the precursor $\text{Na}_2\text{Ti}_3\text{O}_7$ were refined by the Rietveld analysis using the XRD data to be $a = 9.1335(5)$ \AA , $b = 3.8039(2)$ \AA , $c = 8.5718(4)$ \AA , and $\beta = 101.603(5)^\circ$. These values were in good agreement with those in the recent report,⁸ $a = 9.1312(3)$ \AA , $b = 3.8040(1)$ \AA , $c = 8.5687(3)$ \AA , and $\beta = 101.603(3)^\circ$. The chemical composition of $\text{Na}_2\text{Ti}_3\text{O}_7$ was determined by ICP. The Na/Ti ratio was consistent with the stoichiometric $\text{Na}_2\text{Ti}_3\text{O}_7$ composition.

The product after Na^+/H^+ ion exchange experiments was also identified to be a single phase of $\text{H}_2\text{Ti}_3\text{O}_7$, monoclinic

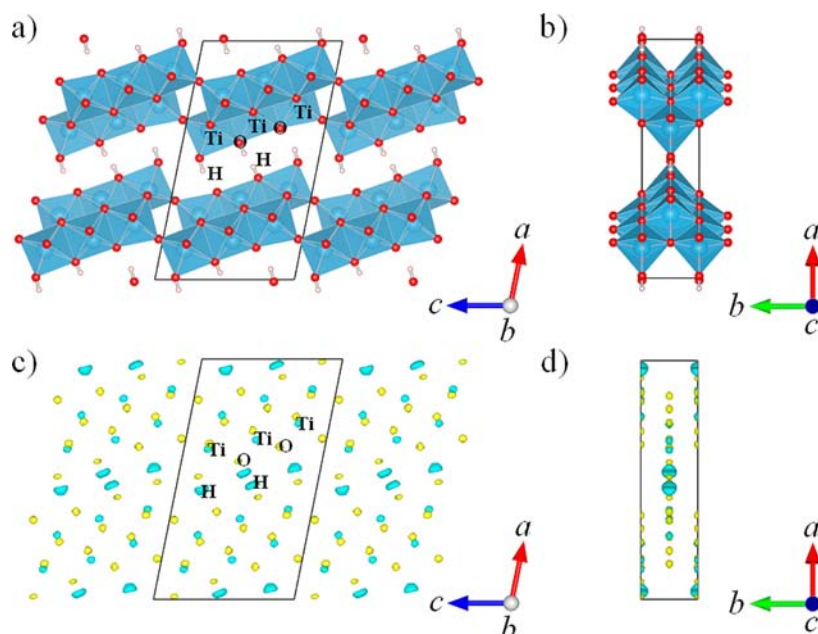


Figure 3. (a, b) Crystal structure of $\text{H}_2\text{Ti}_3\text{O}_7$ viewed along the $[0\ 1\ 0]$ and $[0\ 0\ 1]$ directions. The solid box indicates the unit cell. (c, d) Three-dimensional nuclear scattering length density distribution with an iso surface level in $1.0\ \text{r}\ \text{\AA}^{-3}$ for $\text{H}_2\text{Ti}_3\text{O}_7$ viewed along the $[0\ 1\ 0]$ and $[0\ 0\ 1]$ directions, respectively. The solid box indicates the unit cell. The distribution is colored with blue (gray) or yellow (white) to show a negative or positive nuclear scattering length, respectively.

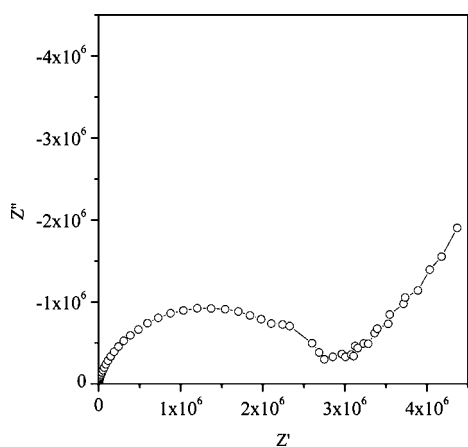


Figure 4. Nyquist plot of the ac impedance spectrum of $\text{H}_2\text{Ti}_3\text{O}_7$.

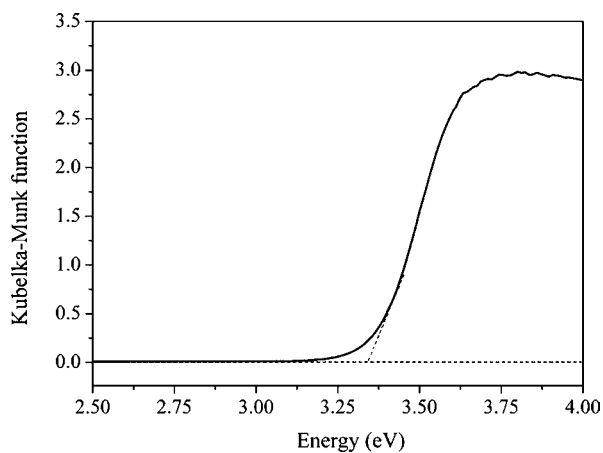


Figure 5. UV-vis absorption spectrum of $\text{H}_2\text{Ti}_3\text{O}_7$.

crystal system, and confirmed the space group $C2/m$. The lattice parameters were refined by the Rietveld analysis using the XRD data to be $a = 16.018(6)\ \text{\AA}$, $b = 3.7468(1)\ \text{\AA}$, $c = 9.1831(4)\ \text{\AA}$, and $\beta = 101.417(3)^\circ$. These values were in good agreement with those in the previous report [6], $a = 16.03(2)\ \text{\AA}$, $b = 3.75(1)\ \text{\AA}$, $c = 9.19(1)\ \text{\AA}$, and $\beta = 101.45(1)^\circ$.⁶ Chemical analysis confirmed that the residual Na contents were less than 0.02 wt %, the value of which was within the experimental error of the analysis.

Crystal Structure of $\text{H}_2\text{Ti}_3\text{O}_7$. The $(\text{Ti}_3\text{O}_7)^{2-}$ framework structure of $\text{H}_2\text{Ti}_3\text{O}_7$ was first examined using powder XRD data. Then, the crystal structure analysis of $\text{H}_2\text{Ti}_3\text{O}_7$ using the powder ND data was initiated with the prerefined $(\text{Ti}_3\text{O}_7)^{2-}$ framework structure (Figure 1). The hydrogen site was determined using the difference Fourier synthesis map using the powder ND data. Figures 1 show the difference Fourier synthesis maps of the $y = 0$ and $y = 0.5$ sections, respectively. The negative residual nuclear scattering length density can be clearly observed at the $4i$ position, suggesting the H occupation. Therefore, the H atom was introduced to the structure model in the following refinement. Finally, the profile function parameters and all structure parameters of $\text{H}_2\text{Ti}_3\text{O}_7$ were refined using the isotropic atomic displacement parameters. Difference Fourier syntheses using the final atomic parameters showed no significant residual peaks. Figure 2 shows the observed, calculated, and difference peaks patterns for the Rietveld refinement of $\text{H}_2\text{Ti}_3\text{O}_7$ using the powder ND data. The resultant reliability values were $R_{\text{wp}} = 2.60\%$ and $R_{\text{p}} = 1.97\%$ with a fit indicator of $\text{GOF} = R_{\text{wp}}/R_{\text{e}} = 1.90$. The lattice parameters for the $\text{H}_2\text{Ti}_3\text{O}_7$ were refined by the Rietveld refinement using the powder ND data to be $a = 16.0380(8)\ \text{\AA}$, $b = 3.7533(1)\ \text{\AA}$, $c = 9.1982(3)\ \text{\AA}$, and $\beta = 101.414(3)^\circ$. The final atomic coordinates and isotropic atomic displacement parameters determined by Rietveld refinement using the powder ND data are listed in Table 1. The selected bond distances are shown in Table 2.

The crystal structure and NSLDD of $\text{H}_2\text{Ti}_3\text{O}_7$ are shown in Figure 3. The basic $(\text{Ti}_3\text{O}_7)^{2-}$ framework in $\text{H}_2\text{Ti}_3\text{O}_7$ is basically the same as those in the previous reports.⁶ All of the three-type TiO_6 octahedra were strongly distorted, and the Ti–O distances were in the wide range of 1.61(1)–2.29(2) Å. These features for the $(\text{Ti}_3\text{O}_7)^{2-}$ unit were very similar to those observed in precursor $\text{Na}_2\text{Ti}_3\text{O}_7$ and Li ion exchange material $\text{Li}_2\text{Ti}_3\text{O}_7$.⁸ However, the difference in layer stack and space group among $\text{Na}_2\text{Ti}_3\text{O}_7$ and $\text{H}_2\text{Ti}_3\text{O}_7$ is clearly ascertained based on the shape of the layered space. These structural change may be caused by difference in ion radius, repulsive force of H1–H1' and the hydrogen bonding O4–H2...O2' across the layer space. The structural stability around the H1, H2, Ti1, Ti2, and Ti3 atoms in $\text{H}_2\text{Ti}_3\text{O}_7$ was examined by bond valence sums. The calculated bond valence sums of H1, H2, Ti1, Ti2, and Ti3 were +1.04(2), +1.03(2), +3.91(5), +4.45(9), and +4.03(5), respectively. Then, the parameters that were used for the calculation of bond valence sum are Ti–O, $\text{BV} - \rho_0 = 1.815$, $\text{BV} - \text{B} = 0.37$; and H–O, $\text{BV} - \rho_0 = 0.569$, $\text{BV} - \text{B} = 0.94$. The bond valence sum value of H1, H2, Ti1, and Ti3 are well-consistent with the formal valence state of H^+ and Ti^{4+} . This fact suggests the ordered occupation of the H atoms in the structure. However, the value of Ti2 is larger than that of Ti^{4+} . We often estimate that frame structure is distorted by ion exchange. As a result, bond length of Ti2–O2 is shorter than the others and the value of the bond valence sum of Ti2 became larger than the valence of Ti^{4+} .

Physical Properties. Figure 4 shows ac impedance plot of the pressed powder samples for $\text{H}_2\text{Ti}_3\text{O}_7$ at room temperature. The tail of impedance plot at a low-frequency side indicates the blocking of the electrode for mobile protons. The impedance plot at a high-frequency side shows single semicircle behavior. The conductivity could not be separated into bulk and grain boundary in the present experiment. The total proton conductivity in $\text{H}_2\text{Ti}_3\text{O}_7$ was $\sigma_{\text{total}} = 1.25 \times 10^{-7} \text{ S cm}^{-1}$ at room temperature. However, we considered influence interparticle, grain boundary, the adsorbed water is large in this measurement. We are now trying to measure the conductivity of $\text{H}_2\text{Ti}_3\text{O}_7$ at high temperatures by low temperature sintered compact.

Figure 5 shows the UV–vis absorption spectrum of $\text{H}_2\text{Ti}_3\text{O}_7$ measured at room temperature. The estimated band gap for $\text{H}_2\text{Ti}_3\text{O}_7$ is about 3.36 eV, the value of which is very similar to those for $\text{Na}_2\text{Ti}_6\text{O}_{13}$ and $\text{Li}_2\text{Ti}_6\text{O}_{13}$, as reported previously.¹³

CONCLUSIONS

In the present study, hydrogen titanium oxide, $\text{H}_2\text{Ti}_3\text{O}_7$, was successfully prepared from $\text{Na}_2\text{Ti}_3\text{O}_7$ as a parent compound via Na^+/H^+ ion exchange in acidic solution at 333 K. The phase purity and chemical composition of the ion-exchanged samples were well-characterized. The crystal structure of $\text{H}_2\text{Ti}_3\text{O}_7$ was refined by Rietveld refinement using the powder neutron diffraction data. The hydrogen site in the tunnel space was successfully refined with the strict H1–O3 and H2–O4 distances of 0.80 and 0.86 Å in $\text{H}_2\text{Ti}_3\text{O}_7$, respectively. The structural validity was confirmed by bond valence sums calculation. The AC impedance measurement revealed that $\text{H}_2\text{Ti}_3\text{O}_7$ was one of the protonic conductors among the hydrogen titanate compounds for the first time.

The low-temperature synthetic techniques such as ion-exchange reaction called “chimie douce” have resulted in major developments in the field of the solid-state chemistry of transition-metal oxides. In many cases, the framework

structures of the parent compounds were maintained nearly unchanged; however, the local structural changes around alkali or hydrogen atoms were recently revealed by the precise structural studies.⁸ In the trititanate $\text{A}_2\text{Ti}_3\text{O}_7$ family with $\text{A} = \text{Na}$, Li , and H , the $(\text{Ti}_3\text{O}_7)^{2-}$ framework in $\text{H}_2\text{Ti}_3\text{O}_7$ that is different from other materials revealed.⁶ This change in the framework, we consider that it caused for hydrogen ion is smaller than the other ions. The difference in the local alkali or hydrogen position among the $\text{A}_2\text{Ti}_3\text{O}_7$ compounds may determine the reactivity in these solid compounds.

ASSOCIATED CONTENT

Supporting Information

Crystallographic information of $\text{H}_2\text{Ti}_3\text{O}_7$ in CIF format. This material is available free of charge via the Internet at <http://pubs.acs.org>.

AUTHOR INFORMATION

Corresponding Authors

*E-mail: kataoka-kunimitsu@aist.go.jp

*E-mail: j.akimoto@aist.go.jp

Notes

The authors declare no competing financial interest.

ACKNOWLEDGMENTS

We thank Dr. Y. Kumashiro and Mr. T. Sotokawa of Ishihara Sangyo Kaisha, Ltd. for the ICP-OES analysis.

REFERENCES

- (1) Le Bail, A.; Fourquet, J. L. *Mater. Res. Bull.* **1992**, *27*, 75–85.
- (2) Corcoran, D. J. D.; Tunstall, D. P.; Irvine, J. T. S. *Solid State Ionics* **2000**, *136–137*, 297–303.
- (3) Orera, A.; Azcondo, M. T.; García-Alvarado, F.; Sanz, J.; Sobrados, I.; Rodríguez-Carvajal, J.; Amador, U. *Inorg. Chem.* **2009**, *48*, 7659–7666.
- (4) Izawa, H.; Kikkawa, S.; Koizumi, M. *J. Phys. Chem.* **1982**, *86*, 5023–5026.
- (5) Izawa, H.; Yasuda, F.; Kikkawa, S.; Koizumi, M. *Chem. Lett.* **1985**, 1775–1778.
- (6) Feist, T. P.; Davies, P. K. J. *Solid State Chem.* **1992**, *101*, 275–295.
- (7) Akimoto, J.; Chiba, K.; Kijima, N.; Hayakawa, H.; Hayashi, S.; Gotoh, Y.; Idemoto, Y. *J. Electrochem. Soc.* **2011**, *158*, A546–A549.
- (8) Chiba, K.; Kijima, N.; Takahashi, Y.; Idemoto, Y.; Akimoto, J. *Solid State Ionics* **2008**, *178*, 1725–1730.
- (9) Petříček, V.; Dušek, M.; Palatinus, L. *Jana2006. The Crystallographic Computing System*; Institute of Physics: Praha, Czech Republic, 2006.
- (10) Ohoyama, K.; Kanouchi, T.; Nemoto, K.; Ohashi, M.; Kajitani, T.; Yamaguchi, Y. *Jpn. J. Appl. Phys.* **1998**, *37*, 3319–3326.
- (11) Izumi, F.; Dillania, R. A. *Recent Research Developments in Physics*; Transworld Research Network: Trivandrum, India, 2002; Vol. 3, part II, pp 699–726.
- (12) Momma, K.; Izumi, F. *J. Appl. Crystallogr.* **2008**, *41*, 653–658.
- (13) Kataoka, K.; Awaka, J.; Kijima, N.; Hayakawa, H.; Ohshima, K.; Akimoto, J. *Chem. Mater.* **2011**, *23*, 2344–2352.